Article

A Simultaneous Analysis of the User Safety and Resilience of a Twin-Tube Road Tunnel

Ciro Caliendo *, Gianluca Genovese and Isidoro Russo

Department of Civil Engineering, University of Salerno, 84084 Fisciano, SA, Italy; ggenovese@unisa.it (G.G.); isrusso@unisa.it (I.R.)
* Correspondence: ccaliendo@unisa.it; Tel.: +39-(89)-964-140

Abstract: This study complements our previous work with a simultaneous analysis of user safety and road tunnel resilience. We developed a computational fluid dynamics (CFD) model and simulated the corresponding egress process to evaluate the risk level of users exposed to different types of fire, such those which might occur on the undisrupted lane of a partially closed tube tunnel due to a traffic accident, or in the adjacent tube when used for two-way traffic in the case of the complete closure of the tube involved in the accident. The CFD results showed that: (i) better environmental conditions were found with the partial closure of the tube rather than the complete one; (ii) additional benefits can be achieved by activating variable message signs (VMSs) that suggest an alternative itinerary for heavy good vehicles (HGVs) only; (iii) safety issues for human health may arise only in the case of a 100 MW fire, occurring during the complete closure of the tube and the use of the parallel one for two-way traffic. The findings of the CFD simulations were subsequently used to perform a quantitative risk analysis (QRA) based on a probabilistic approach. The findings of the QRA were found to be consistent with those obtained by the tunnel resilience analysis. In particular, the lowest risk level for user safety was found with the partial closure of the tube instead of the complete one, and by activating the VMSs to redirect HGVs only towards an alternative itinerary. This finding was found to correspond to a higher resilience index of the tunnel (i.e., a lower resilience loss due to a traffic accident occurring in a tube). This study increases our knowledge on certain relevant aspects of the operating conditions of tunnels and can serve as a possible reference for tunnel management agencies (TMAs) in their choice of the most appropriate arrangement to recover the functionality of a tunnel taking into account both user safety and resilience at the same time.

Keywords: road tunnels; user safety; resilience index; recovery strategies; computational fluid dynamics; quantitative risk analysis

1. Introduction

Considerable research has been carried out over the last few decades to better understand the factors that affect the occurrence of traffic accidents in road tunnels. These studies have led to the development of several statistical models to estimate the expected value of accident frequency (i.e., number of crashes per year) [1–6] as a function of geometry, traffic flow, and certain types of equipment implemented in tunnels.

The occurrence of traffic accidents in a road tunnel might also temporarily compromise its functionality over time due to the partial or complete closure of the tunnel (e.g., only one lane or all the lanes of the tunnel are closed), as well as this potentially causing negative effects on the service level of the traffic flow of the road network containing the tunnel. The duration of the disruptive event in the tunnel may depend on how serious it is. When there is a severe accident (i.e., involving fatalities and/or injuries), it might also take up to several hours before the tunnel is available again for traffic flow. This may be due to the time necessary for the rescue team to arrive, the road police to investigate the causes on site, the local emergency services to help the injured or take away fatalities, and the tunnel management staff to remove damaged vehicles and clean the road of any debris.

Given the essential role that road tunnels play in a road network in supporting the mobility of people and goods, following a traffic accident, the non-availability of a tunnel for the passage of traffic flow through it is a relevant issue for the social and economic interests of the community.

Road tunnels that present an adaptive response to a disruptive event (e.g., a traffic accident) are generally described as resilient. There is no shared concept of resilience in the current literature. However, with respect to infrastructure networks, resilience may be described as "the ability of a system to rapidly recover its functionality after a disturbing event" [7].

Resilience of a transportation system has been investigated from different perspectives. Some researchers, for example, have discussed the most appropriate metrics for assessing the resilience of an infrastructure network [7–10]. Knoop et al. [11], and Liao et al. [12] focused, instead, on traffic flow simulation models to investigate both the robustness of a road system as well as the effectiveness of different management strategies. Omer et al. [13], and Antoniou et al. [14] proposed frameworks to evaluate the resilience of a road network. Reggiani et al. [15] concentrated on the resilience and vulnerability of transportation networks. Kaviani et al. [16] found the optimal location of road guidance tools for re-routing vehicular flow after a disturbing event. Amini et al. [17] developed a methodology to evaluate the effectiveness of diversion on the resilience of a road network. Xu et al. [18] investigated the redundancy of a transportation network, while Sohouenou and Neves [19] concentrated on both the robustness of a network and the rapidity of the recovery process. Abudayyeh et al. [20] proposed a method for setting traffic signals in order to improve resilience. Khetwal et al. [21] set up a stochastic simulation model to evaluate tunnel resilience, while Zhao [22] developed a genetic algorithm for optimizing a road network. PIARC [23] presented the current state of knowledge of road tunnel resilience, whereas Borghetti et al. [24] investigated the resilience and emergency management of road tunnels. Finally, Caliendo et al. [25] set up a traffic simulation model for evaluating the resilience of a twin-tube motorway tunnel in the case of a traffic accident in a tube.

However, it is worth highlighting that, among the studies referred to, only a few have focused specifically on the resilience of road tunnels, such as Liao et al. [12], Khetwal et al. [21], PIARC [23], Borghetti et al. [24], and Caliendo et al. [25].

Moreover, as far as the authors of this paper are aware, there are no studies in the current literature in which the restoration of the functionality of a tunnel (i.e., resilience) in the event of a traffic accident is also associated with user safety that might be compromised, for example, by a fire of vehicles transiting on the remaining undisrupted lanes of the partially closed tunnel. Furthermore, in the case of a twin-tube road tunnel in which a tube is completely closed due to a traffic accident, the resilience of the tunnel system has not been evaluated in combination with occupant safety that may be affected by a fire affecting vehicles that, having changed carriageway, use one lane of the adjacent tube to travel (i.e., where bi-directional traffic conditions are generated in the parallel tube). This represents a lacuna of knowledge that this paper seeks to fill.

With reference to our previous studies, it is also worth highlighting that we did not investigate user safety in the earlier paper [25], while in other studies, we evaluated only the safety level of tunnel users in the event of a fire (e.g., Caliendo et al. [26–32], Caliendo and De Guglielmo [33–36], and Caliendo and Genovese [37]), but not resilience. In other words, tunnel resilience and user safety were not coupled to each other; consequently, the effects of a strategy to recover the functionality of a tunnel that might influence user safety or vice versa were not considered. A simultaneous analysis of user safety and resilience now represents an important topic of discussion in the field of tunnel engineering, in particular for tunnel management agencies (TMAs). This represents a primary justification for the present research.

This study complements our previous research studies by coupling user safety and tunnel resilience, to provide additional perspectives on relevant factors, as well as to suggest certain recovery strategies in order to enhance the resilience of tunnels without

neglecting user safety. Moreover, it facilitates the dissemination of additional information for road tunnel management.

A twin-tube motorway tunnel was investigated. We developed two computational fluid dynamics (CFD) models for scenarios of the partial or complete closure of a tube; then, the corresponding evacuation processes were simulated to evaluate exposure risk to users due to different types of fire. The results obtained were applied in a quantitative risk analysis (QRA), based on a probabilistic approach, to build F-N curves for each scenario investigated. Comparisons between the F-N curves and tunnel resilience were carried out to optimize the choice of recovery strategy in relation to user safety.

Given that it was not obvious how the implementation of certain recovery measures for improving the tunnel resilience might simultaneously combine with user safety in the event of a fire, we reviewed our assumptions with a view to obtaining a deeper understanding of both safety and resilience at the same time.

In the light of the above considerations, it needs to be stressed that the main objective of the present study was to couple a resilience analysis of twin-tube road tunnels with a risk assessment for users in the event of a fire that might occur during the partial or complete closure of a tube. The findings might be useful for understanding whether the recovery strategies implemented to restore the functionality of the system in the event of a traffic accident in a road tunnel are suitable also from the point of view of user safety.

The scientific significance of the present study lies in the improvement of knowledge in the field of both fire safety engineering and tunnel management, by providing additional insights on both user safety and tunnel resilience, and in the dissemination of further information for the operating conditions of tunnels in the event of emergency.

The paper is organized as follows: the next section contains a description of the tunnel investigated. Subsequently, the computational fluid dynamics (CFD) modeling and people egress process are presented and implemented. Then, the quantitative risk analysis (QRA) is described, and the frequency (F) of potential fatalities (N) is quantified. The results are then reported and commented on, and comparisons are made with tunnel resilience for the different scenarios investigated. Finally, some conclusions are drawn and recommendations for practical applications are made, and future research possibilities are discussed.

2. Materials and Methods

2.1. Tunnel Description

A twin-tube motorway tunnel situated along an Italian road network is examined. Each tube has a length of 850 m and is used for one-way traffic under ordinary conditions of service. The tubes are flat, straight, and have no emergency lanes. Each tube is characterized by a horseshoe-shaped cross-section of 55 m^2, with a total width of 9.5 m (i.e., two traffic lanes of 3.5 m, and two sidewalks of 1 m) and a maximum height of 6.8 m. An emergency exit, which consists of a cross-connection between the two tubes, is located in the middle of the tunnel length.

2.2. Scenarios Investigated

In our previous study [25], we assumed that the occurrence of a traffic accident in the north tube would lead to different potential scenarios involving its partial or complete closure for 1 h, 2 h, or 3 h (however, in this investigation, we considered the worst-case scenario, which was a closure of 3 h). Specifically, the functionality of the investigated twin-tube motorway tunnel, after the occurrence of a traffic accident in the north tube, was assumed to be restored by utilizing the remaining available lane of the north tube (i.e., only one lane is closed) or rearranging the traffic flow using the south tube for two-way traffic (i.e., both lanes of the north tube are closed). The effects of the presence of an alternative route, along which to divert heavy goods vehicles (HGVs), were also investigated.

In this study, we investigated the same scenarios assuming that, during the partial or complete closure of the north tube due to the occurrence of a traffic accident in it, a fire had simultaneously occurred on the undisrupted remaining lane of the north tube, or in the

parallel tube used for two-way traffic, in the case of the partial or complete closure of the north tube.

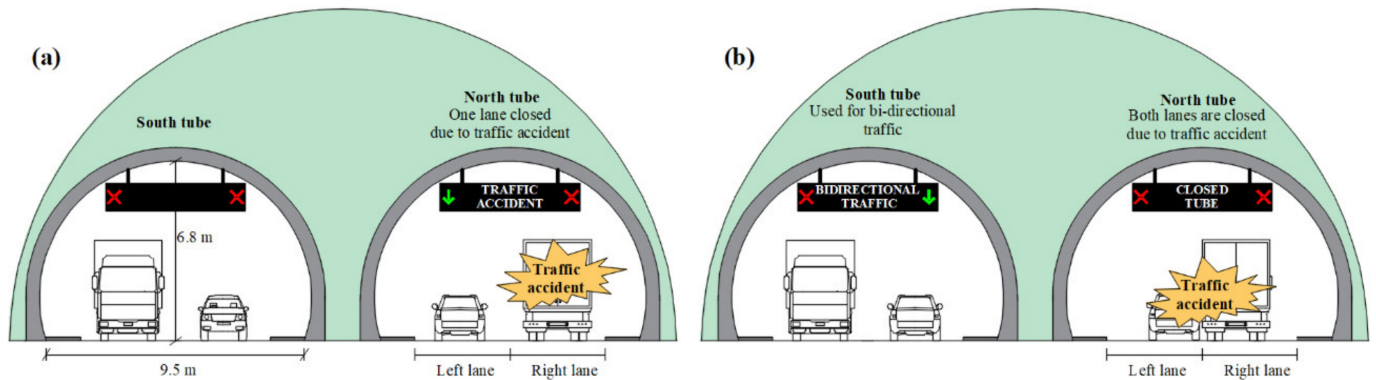Figure 1 shows a cross-section of the twin-tube motorway tunnel examined.

Figure 1. Cross-section of the twin-tube motorway tunnel examined when: (**a**) only one lane of the north tube is closed due to a traffic accident, (**b**) both lanes of the north tube are closed due to a traffic accident.

Figure 2 shows the scenarios investigated: (i) Scenario 0 represents the case in which the tunnel system is used under its ordinary conditions of functionality (i.e., without any traffic accident and with both lanes of each tube used for one driving direction) when a fire occurs in the north tube; (ii) Scenario Ia corresponds to the case in which, assuming that the north tube is partially closed due to a traffic accident on the right lane, a fire occurs on the undisrupted remaining lane of the north tube (i.e., the left lane); (iii) Scenario Ib is similar to Scenario Ia, but also includes the use of an alternative route along which, by using variable message signs (VMSs), only HGVs traveling towards the north are diverted; (iv) Scenario IIa corresponds to the case of the complete closure of the north tube and the use of the parallel tube for two-way traffic; here, the fire is assumed to occur on the lane used by the traffic flow traveling towards the north; (v) Scenario IIb is similar to Scenario IIa, but it also includes the use of an alternative route along which, using VMSs, only HGVs traveling towards the north are redirected. With reference to Scenarios IIa and IIb, the two traffic by-passes located at the tunnel portals, which allow for a change of carriageway, are assumed to be opened by the emergency service team in a very short time (i.e., 10 min) from the start of the traffic accident. The nodes E and I represent the two motorway junctions which are before the portals of the twin-tube tunnel that was investigated. Specifically, node E is used by HGVs when the alternative itinerary is recommended for these vehicles only.

2.3. Hourly Traffic Volume

The traffic flow, expressed in terms of hourly traffic volume (VHP), transiting through the north tube during its ordinary conditions of functionality (i.e., Scenario 0) was found to be—according to the traffic database of the road management agency—equal to 2200 vehicles/h (i.e., 1100 vehicles/h per lane). However, it should be noted that the partial or complete closure of the north tube due to a traffic accident might lead to traffic congestion on its remaining undisrupted lane or in the adjacent tube used for two-way traffic, respectively. On this basis, the VHP was assumed to be equal to the capacity of a one-way lane (i.e., 1700 vehicles/h) or to that of a bi-directional carriageway having two lanes (i.e., 3200 vehicles/h) [38] for the partial (i.e., Scenarios Ia and Ib) or complete (i.e., Scenarios IIa and IIb) closure of the north tube, respectively. The heavy vehicle percentage (i.e., buses and HGVs), which was obtained from the same traffic database, was always equal to 25%.
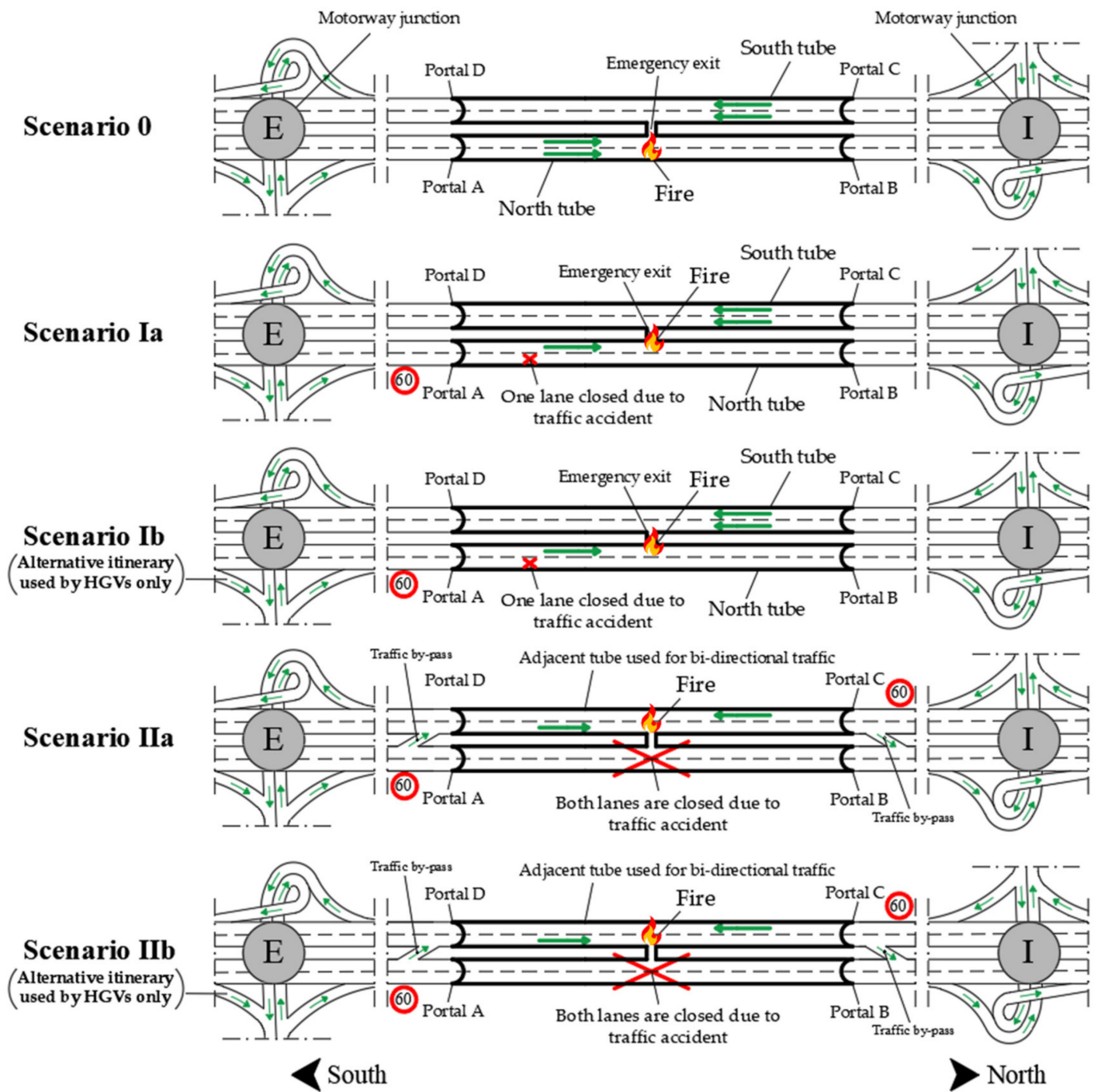
Figure 2. Schematic illustration of the scenarios investigated. Scenario 0: ordinary conditions of functionality of the tunnel system (i.e., both lanes of each tube are used for one driving direction) with a fire that occurs in the north tube; Scenario Ia: partial closure of the north tube (i.e., only the right lane is closed due to a traffic accident) with a fire that might occur on the left lane of the north tube; Scenario Ib: similar to Scenario Ia, but with the HGVs traveling towards the north tube diverted to an alternative itinerary; Scenario IIa: complete closure of the north tube (i.e., both lanes are closed due to a traffic accident) with a fire that might occur on the lane of the adjacent tube that is used by traffic traveling towards the north; Scenario IIb: similar to Scenario IIa, but with the HGVs traveling towards the north tube diverted to an alternative itinerary.

2.4. Types of Burning Vehicles

The effects of five different categories of burning vehicles were investigated. Each burning vehicle was assumed to be placed in five different positions along the right lane of the north tube in Scenario 0 (i.e., 145, 280, 420, 570, and 710 m from portal A). The burning vehicles were assumed to be two cars, a van, a bus, and two different types of HGVs capable of developing a maximum heat release rate (HRR_{max}) of 8, 15, 30, 50, and 100 MW, respectively. The same five different types of burning vehicles and locations were considered on the remaining undisrupted lane (i.e., the left lane) of the north tube, partially closed due to a traffic accident in Scenario Ia; while in Scenario Ib only the occurrence of a fire involving light vehicles was simulated (i.e., characterized by an HRR_{max} of 8 and 15 MW) since the HGVs were redirected to the alternative route.

In the case of the complete closure of the north tube and the use of the parallel tube for two-way traffic, the aforementioned five different types of burning vehicles were assumed to be located on the lane used by traffic traveling towards the north and at the aforementioned positions (i.e., 145, 280, 420, 570, and 710 m from portal D) in Scenario IIa; while in Scenario IIb, only light vehicles were considered (i.e., HRR_{max} of 8 and 15 MW) given that the HGVs were diverted to the alternative itinerary.

2.5. Natural Ventilation

The two tubes are not equipped with a mechanical ventilation system. Therefore, the longitudinal ventilation along each tube is natural and due to the piston effect of moving vehicles. In this respect, the natural ventilation was simulated by setting an appropriate pressure difference between the tunnel portals. Specifically, a positive pressure difference of 5 Pa [29] was applied between the entrance portal (portal A) and the exit portal (portal B) of the north tube when used for unidirectional traffic towards the north.

In the case of the complete closure of the north tube and the use of the parallel tube for two-way traffic, due to the two opposite traveling directions in the tube, the piston effect is expected to be almost negligible. However, since the speed of the vehicles that changed tube is expected to be slightly lower than that of the vehicles traveling in the opposite direction, a negative pressure difference of −0.5 Pa [30] was set for traffic flow traveling towards the north (i.e., from portal D to portal C of the adjacent tube).

2.6. Concrete Characteristics

The tunnel walls and ceiling were assumed to be made of ordinary concrete with a thickness of 0.4 m. The properties of this material, which were taken from the literature, are as follows: thermal conductivity of 1.67 W/m/K, specific heat of 0.94 kJ/kg/K, density of 2585 kg/m^3, and emissivity of 0.9 [39].

2.7. Results of Resilience Analysis

Resilience analysis of a transportation system is generally performed using traffic simulation models [40–44]. In our previous study [25], the level of functionality of the twin-tube motorway tunnel, during the period in which the north tube was partially or completely closed due to a traffic accident, was calculated as the ratio between the average travel time before and after the traffic accident. We calculated the reduction in the functionality F* (%) for all the scenarios examined (the functionality level F* was assumed to be equal to 100% in absence of incidents). Then, we built the functionality curves vs. time (i.e., F* (%) − t) and for all the scenarios computed the resilience loss: $R_{LOSS} = \int_{t_0}^{t_h} [100 - F^*(t)]dt$, in which t_o is the time instant when the traffic accident occurs in the north tube and t_h is the time instant when the twin-tube tunnel is again fully functional. Smaller resilience losses were found with the partial closure of the north tube rather than the complete one. However, when an alternative route was activated for HGVs only, both in the event of the partial and of the complete closure of the north tube, minor reductions of resilience losses were found compared to those without considering HGV rerouting.

In order to describe the resilience through a parameter, whose value ranges between 0 and 1, we computed the resilience index ($R(t_h) = \frac{\int_{t_0}^{t_h} F^*(t)dt}{t_h - t_0}$) that is widely used in the literature for transportation networks. A low resilience index denotes a high resilience loss (i.e., a resilience index equal to one corresponds to a zero-resilience loss). The resilience index confirmed the abovementioned findings of the resilience loss in all the scenarios investigated.

Given these findings, the intent of this paper was to assess the impacts on user safety related to each of the mentioned fire scenarios in order to help tunnel management agencies (TMAs) decide which arrangement is more appropriate to adopt in the case of a traffic accident in a tube of a twin-tube road tunnel.

2.8. Research Framework

This study is set in the context of research on the simultaneous analysis of user safety and resilience of road tunnels, but expands the state-of-the-art by setting up a computational fluid dynamics (CFD) model to assess the risk exposure of users during their escape from the tunnel in the event of a fire occurring after a traffic accident had occurred, as well as estimating the corresponding potential number of victims with a probabilistic-based quantitative risk analysis (QRA). Therefore, given the lack of studies in which resilience is associated with user safety in road tunnels, this paper can serve as a possible reference for tunnel management agencies (TMAs), and a means of improving our knowledge in the field of the interaction between the recovery of the functionality of tunnels and user safety.

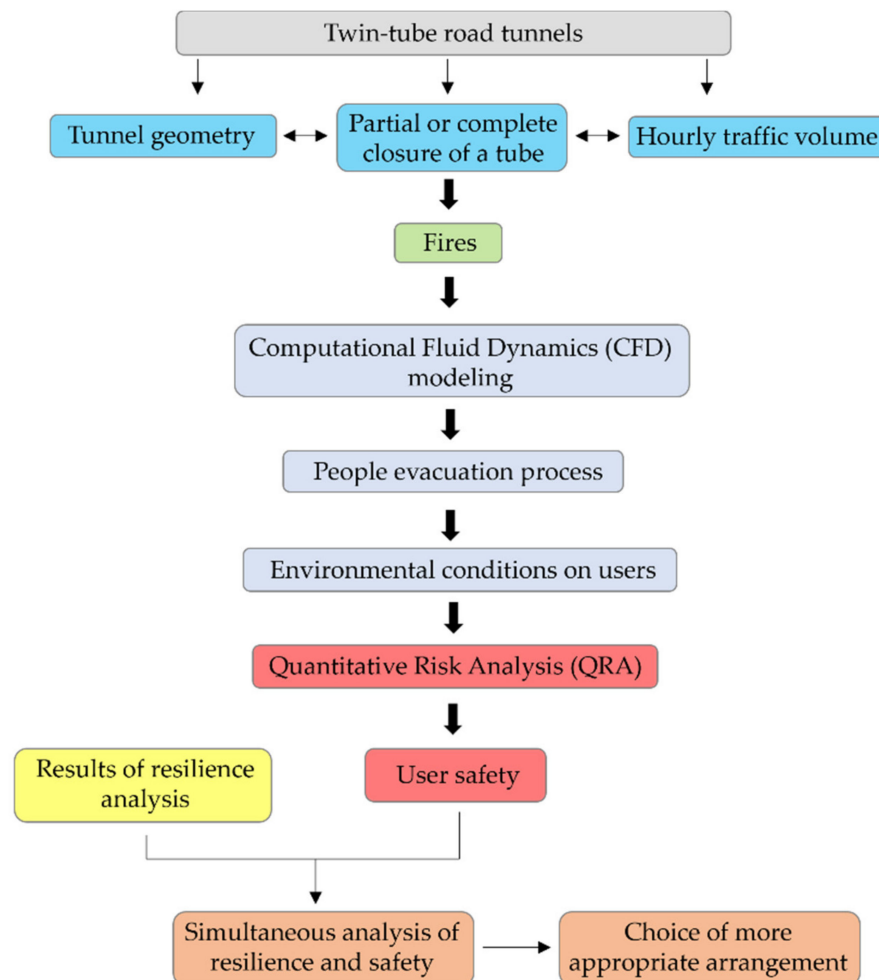The methodology applied is briefly represented in Figure 3.

Figure 3. Flowchart of the methodology.

3. CFD Modeling

3.1. Fire Simulation Code

Computational fluid dynamics (CFD) modeling is the most suitable tool for reproducing a fire; some of its applications, with reference to road tunnels, can be found in Caliendo et al. [25–31]. In this paper, the Fire Dynamics Simulator (FDS) version 6.7.3 [45], which has been widely reported in the literature regarding the simulation of fires in road tunnels, was used as a CFD code. It is an open-source fire-driven fluid flow model developed in collaboration between the VTT Technical Research Centre of Finland and the National Institute of Standards and Technology (NIST).

3.2. Physical Modeling

The FDS code solves the Navier–Stokes equations, coupled with the physical sub-models of turbulence, combustion, and thermal radiation, in each three-dimensional grid in which the computational domain is discretized. The combustion, turbulence, and radiation models for the FDS application are described in detail in the FDS user's guide [45]. The accuracy of the results (e.g., temperature, velocity and direction of air flow, smoke and toxic gas concentration) provided by the FDS code depends on several factors, the most important of which concerns the fire, physical sub-models, and mesh resolution. The main input data to simulate tunnel fire scenarios using the FDS code are related to the following: tunnel geometry, position and dimensions of the burning vehicle, HRR growth law, yields of combustion products, location and geometry of queued vehicles, and the pressure difference between tunnel portals to reproduce the longitudinal ventilation.

3.3. Fire Growth Phases

In our CFD modeling, each burning vehicle (i.e., car, van, bus, and HGV) was geometrically represented as a parallelepiped and was described in terms of both maximum heat release rate (HRR_{max}) and time (t_{max}) to reach the maximum HRR. With reference to each fire curve, a linear law was considered for the fire growth phase (i.e., HRR_{max} = 8 MW is achieved according to a linear increase after t_{max} = 5 min from the fire start; HRR_{max} = 15 MW and HRR_{max} = 30 MW are reached according to a linear increase after t_{max} = 7 and t_{max} = 9 min from the fire start, respectively; HRR_{max} = 50 MW and HRR_{max} = 100 MW are both achieved according to a linear increase after t_{max} = 10 min from the fire start). Each linear increase is then followed by a constant HRR_{max} phase until the arrival of the fire brigade to extinguish the fire. The details regarding the assumptions made for the geometric characteristics of the burning vehicles and the yields of combustion products are reported in Caliendo et al. [29,30].

3.4. Model Validation

The model, for the resolution of which the FDS code was used, was preliminarily validated by simulating a small-scale tunnel fire. Then, its temperature predictions were compared with the experimental temperature data provided by Xue et al. [46]. The simulated temperature showed a good level of conformity with the measured temperatures (i.e., an error of no more than 5%), confirming the ability of the FDS code to correctly reproduce tunnel fire scenarios.

3.5. Sensitivity Analysis

Subsequently, a grid sensitivity analysis was performed to identify the optimal mesh resolution. Based on the results of this analysis, which were discussed in detail in Caliendo et al. [29], the tunnel volume was discretized with 1,095,255 cubic cells of 0.4 m side.

4. Evacuation Modeling

4.1. Egress Simulation Code

In this study, the evacuation module of the FDS code, known as Evac [47], was used to simulate the user egress process from the north tube or adjacent tube (depending on the partial or complete closure of the north tube) during each fire. Each user is assumed to be an individual agent with different characteristics and escape strategies (e.g., walking speed, choice of emergency exit, and escape route). Users can move in a 2D space, but their movements are conditioned during the evacuation process by the environmental conditions (i.e., toxic gases) caused by the fire. However, since Evac, which uses the FDS output as an input, accounts for only the risk due to toxic gases, which is expressed in terms of the fractional effective dose known as $FED_{toxic\ gases}$, we also implemented an additional procedure to estimate the effects of the temperature and radiation on evacuating users, which was expressed in terms of FED_{heat}, using the procedure reported in DiNenno et al. [48].

4.2. Queue Formation and People Evacuation

Several FDS + Evac simulations were performed to assess the exposure to risk of the tunnel users under the different fires investigated, each of which involved a certain HRR_{max} and location of the burning vehicle in the tunnel tube. It is worth mentioning that the vehicles in the queue occupy: (i) both lanes of the north tube upstream of the fire for Scenario 0; (ii) the remaining undisrupted lane (i.e., the left lane) of the north tube upstream of the fire for Scenarios Ia and Ib; (iii) both lanes, including one upstream and one downstream of the fire, of the adjacent tube used for two-way traffic for Scenarios IIa and IIb. The number of queued vehicles was computed by assuming that: (i) vehicles in the queue stop without passing the fire; (ii) vehicles queue up one behind the other maintaining a safety distance of 2 m; (iii) the first queued vehicle stops at 10 m from the burning vehicle. Figure 4 shows a schematic layout of the queued vehicles upstream and/or downstream of the burning vehicle for each scenario examined. It should be noted that each tunnel user, initially positioned next to his/her own vehicle, evacuates towards a safe place (portals or emergency exit) using the nearest sidewalk.

The number of users potentially at risk in a tube obviously depends on the number of cars, HGVs, and buses present in the queue. The occupancy rates of the cars and vans, HGVs, and buses were assumed to be equal to 1.7 [28], 1, and 30 people, respectively. Given that the percentage of heavy vehicles was equal to 25% of the traffic flow (i.e., 23% of HGVs and 2% of buses), we estimated an average occupancy rate considering all the vehicles in the queue (i.e., cars, vans, buses, and HGVs) equal to 2 for Scenarios 0, Ia, and IIa; while that related to light vehicles only (i.e., cars and vans) was calculated to be 1.7 for Scenarios IIa and IIb. Obviously, by multiplying the number of queuing vehicles by 2 or 1.7, we were able to estimate the corresponding number of users escaping from the fire for the mentioned scenarios.

It was assumed that, depending on the fire location, the users leave the tunnel by escaping towards the entrance portal (portal A) or the emergency exit (located in the middle of the tunnel length) when the north tube is used for unidirectional traffic (i.e., Scenarios 0, Ia, and Ib); while the users escape from one of the two portals (portals C or D) of the adjacent tube or from the emergency exit when this tunnel tube is employed for two-way traffic (i.e., Scenarios IIa and IIb). With reference to the emergency exit, it should be noted that it was assumed not to be usable by evacuees when the fire source was located in the middle of the tunnel length (i.e., next to the emergency exit).
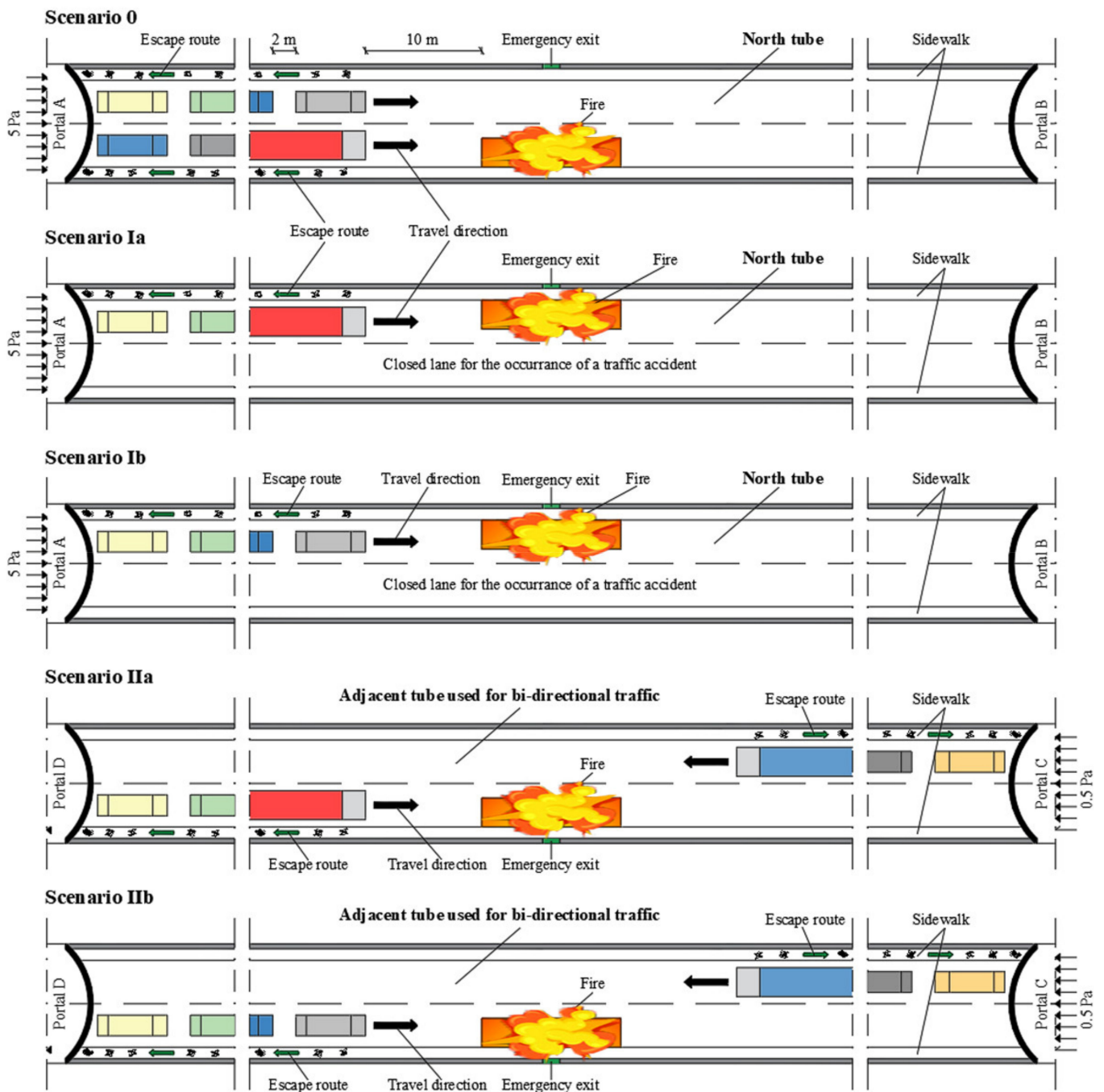
Figure 4. Schematic layout of queued vehicles upstream and/or downstream of the burning vehicle for each scenario examined. Scenario 0: ordinary conditions of functionality of the tunnel system (i.e., both lanes of each tube are used for one driving direction) with a fire that occurs in the north tube; Scenario Ia: partial closure of the north tube (i.e., only the right lane is closed due to a traffic accident) with a fire that might occur on the left lane of the north tube; Scenario Ib: similar to Scenario Ia, but with the HGVs traveling towards the north tube diverted to an alternative itinerary; Scenario IIa: complete closure of the north tube (i.e., both lanes are closed due to a traffic accident) with a fire that might occur on the lane of the adjacent tube that is used by traffic traveling towards the north; Scenario IIb: similar to Scenario IIa, but with the HGVs traveling towards the north tube diverted to an alternative itinerary.

Table 1 shows the number of vehicles in the queue and the number of users escaping from one of the tunnel portals and/or from the emergency exit for each fire location and scenario investigated.

Table 1. Number of vehicles in the queue and number of users escaping from one of the tunnel portals and/or from the emergency exit for each fire location and scenario investigated. Scenario 0: ordinary conditions of functionality of the tunnel system (i.e., both lanes of each tube are used for one driving direction) with a fire that occurs in the north tube; Scenario Ia: partial closure of the north tube (i.e., only the right lane is closed due to a traffic accident) with a fire that might occur on the left lane of the north tube; Scenario Ib: similar to Scenario Ia, but with the HGVs traveling towards the north tube diverted to an alternative itinerary; Scenario IIa: complete closure of the north tube (i.e., both lanes are closed due to a traffic accident) with a fire that might occur on the lane of the adjacent tube that is used by traffic traveling towards the north; Scenario IIb: similar to Scenario IIa, but with the HGVs traveling towards the north tube diverted to an alternative itinerary.

Scenario	Number of Queued Vehicles and Escaping Users	Distance of the Fire Center from the Entrance Portal for Traffic Flow towards the North Direction [m]									
		145		280		420		570		710	
		Upstream	Downstream	Upstream	Downstream	Upstream	Downstream	Upstream	Downstream	Upstream	Downstream
0	Queued vehicles	32	-	66	-	100	-	138	-	172	-
	Escaping users	64	-	132	-	200	-	276 (117)	-	344 (188)	-
Ia	Queued vehicles	16	-	33	-	50	-	69	-	86	-
	Escaping users	32	-	66	-	100	-	138 (59)	-	172 (94)	-
Ib	Queued vehicles	16	-	33	-	50	-	69	-	86	-
	Escaping users	27	-	56	-	85	-	117 (50)	-	146 (80)	-
IIa	Queued vehicles	16	86	33	69	50	51	69	33	86	15
	Escaping users	32	172 (90)	66	138 (56)	100	102	138 (59)	66	172 (94)	30
IIb	Queued vehicles	16	86	33	69	50	51	69	33	86	15
	Escaping users	27	172 (90)	56	138 (56)	85	102	117 (50)	66	146 (80)	30

The number of users that escape from the emergency exit located in the middle of the tunnel length are reported in brackets.

4.3. Movement Times

The movement time of each tunnel user depends on: (i) vehicle queuing time; (ii) the pre-movement time of the user (i.e., the sum of the detection and reaction time); (iii) the walking speed of the user.

The frequency per unit time with which the vehicles enter the tunnel after the start of the fire was considered constant and computed to be equal to 3.27 s for Scenario 0 (VHP = 1100 vehicles/h per lane), 2.12 s for Scenarios Ia and Ib (VHP = 1700 vehicles/h), and 2.25 s for Scenarios IIa and IIb (VHP = 1600 vehicles/h per direction). As a result, the last user escaping from the tube during a fire will be affected by a delay of 1.15 or 1.02 s when the VHP is equal to 1100 vehicles/h per lane rather than 1700 vehicles/h or 1600 vehicles/h per direction, respectively.

The pre-movement time of each user was set to be 1.5 min for 8, 15, 50, and 100 MW fires, while it was increased by 1 min (i.e., 2.5 min in total) in the event of a 30 MW fire to consider the time needed for all the users to exit the bus [49]. Despite the fact that in the FDS modeling the queued vehicles in the tunnel tube are assumed to be stopped when the fire started, the time with which the vehicles enter the tunnel tube was considered in the evacuation model by attributing an extra pre-movement time to each evacuee.

The unimpeded walking speed (i.e., the walking speed that users can assume in the absence of any interference) was assumed to be 0.7 m/s. However, the effective walking speed during a fire might be lower than the unimpeded speed due to reduced visibility distance, very high concentrations of smoke, and the presence of obstacles (e.g., queued vehicles) along the escape routes. The effective walking speed is automatically computed by the Evac code based on the FDS output.

5. CFD Results

Considering the worst-case combination of HRR_{max} (i.e., 100 MW for Scenarios 0, Ia, and IIa, and 15 MW for Scenarios Ib and IIb) and the location of the fire (i.e., in the middle of the tunnel tube length) for each scenario investigated, the longitudinal profiles of

temperature, radiant heat flux, visibility distance, and toxic gases concentration predicted at breathing height (2 m) along the escape route (i.e., the nearest sidewalk) are reported in this section and compared with the acceptable tenability limits in order to verify if the environmental conditions were acceptable for human health.

5.1. Temperature

Figure 5 shows the longitudinal temperature profiles predicted at 2 m height along the escape path after 10 min from the start of the 100 MW (i.e., Scenarios 0, Ia, and IIa) or 15 MW (i.e., Scenarios Ib and IIb) fire located in the middle of the tunnel tube length, as well as the positions occupied by the last escaping user after 10 min of fire exposure both upstream (for all scenarios) and downstream (for Scenarios IIa and IIb only) of the burning vehicle. It is worth noting how the aforementioned evacuee, according to his/her effective walking speed and pre-movement time, reaches a distance upstream of the fire of about 371 m (i.e., walking speed of 0.7 m/s, the red user) for Scenarios 0, Ia, and Ib (escape route only towards portal A of the north tube), as well as for Scenario IIb both upstream and downstream of the fire (i.e., escape route in the direction of both portal D and portal C of the adjacent tube). In contrast, for Scenario IIa, due to a reduced walking speed (i.e., about 0.55 m/s), he/she (the green user) reaches, after 10 min from the start of the fire, a shorter distance from the burning vehicle (i.e., 295 m), which is due to the poor visibility and high CO concentration (see Sections 5.3 and 5.4, respectively). However, the mentioned user is always exposed to a temperature $\leq 60\,°C$ (i.e., dotted line), which is the tenability limit according to UPTUN [50].
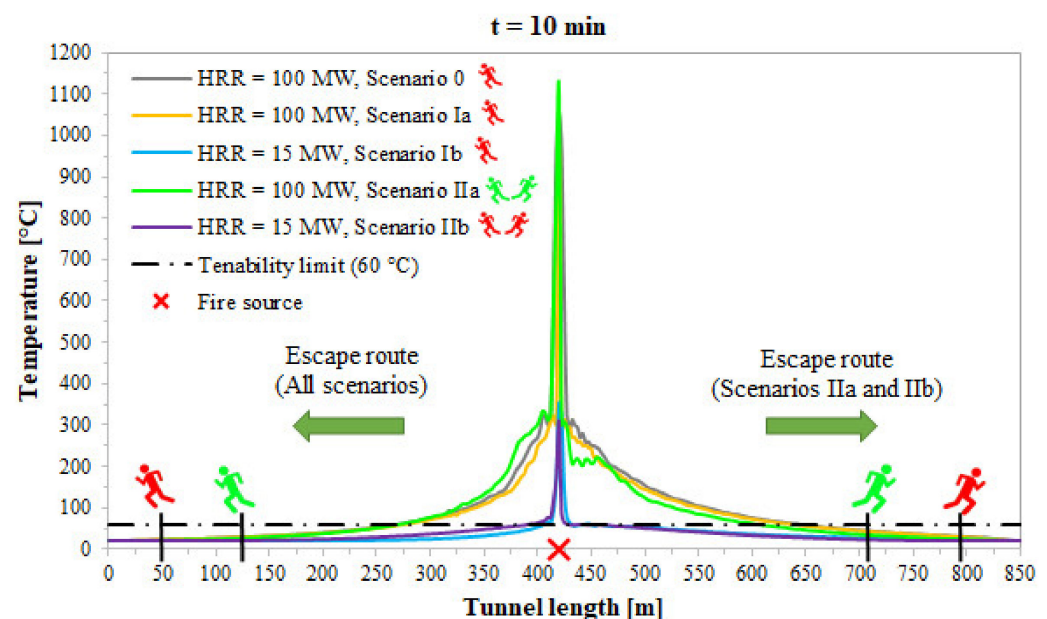

Figure 5. Longitudinal temperature profiles predicted at 2 m height along the escape path after 10 min from the start of the 100 MW (i.e., Scenarios 0, Ia, and IIa) or 15 MW (i.e., Scenarios Ib and IIb) fire located in the middle of the tunnel length. Scenario 0: ordinary conditions of functionality of the tunnel system (i.e., both lanes of each tube are used for one driving direction) with a fire that occurs in the north tube; Scenario Ia: partial closure of the north tube (i.e., only the right lane is closed due to a traffic accident) with a fire that might occur on the left lane of the north tube; Scenario Ib: similar to Scenario Ia, but with the HGVs traveling towards the north tube diverted to an alternative itinerary; Scenario IIa: complete closure of the north tube (i.e., both lanes are closed due to a traffic accident) with a fire that might occur on the lane of the adjacent tube that is used by traffic traveling towards the north; Scenario IIb: similar to Scenario IIa, but with the HGVs traveling towards the north tube diverted to an alternative itinerary.

5.2. Radiant Heat Flux

Figure 6 shows the longitudinal profiles radiant heat flux predicted at 2 m height along the escape path after 10 min from the start of the 100 MW (i.e., Scenarios 0, Ia, and IIa) or 15 MW (i.e., Scenarios Ib and IIb) fire located in the middle of the tunnel length.

Figure 6. Longitudinal profiles of radiant heat flux predicted at 2 m height along the escape path after 10 min from the start of the 100 MW (i.e., Scenarios 0, Ia, and IIa) or 15 MW (i.e., Scenarios Ib and IIb) fire located in 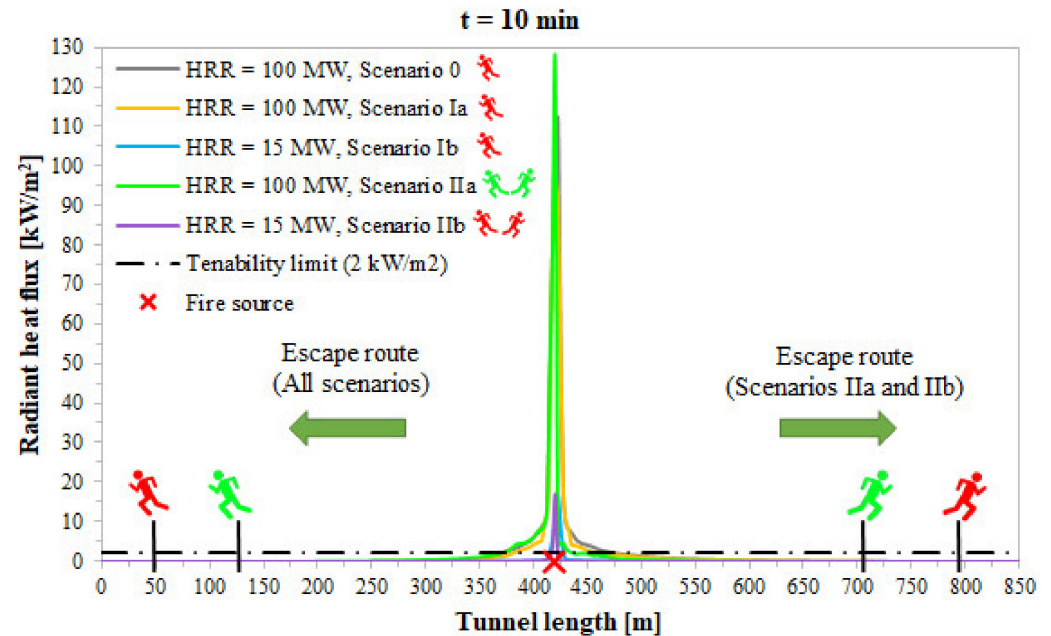the middle of the tunnel length. Scenario 0: ordinary conditions of functionality of the tunnel system (i.e., both lanes of each tube are used for one driving direction) with a fire that occurs in the north tube; Scenario Ia: partial closure of the north tube (i.e., only the right lane is closed due to a traffic accident) with a fire that might occur on the left lane of the north tube; Scenario Ib: similar to Scenario Ia, but with the HGVs traveling towards the north tube diverted to an alternative itinerary; Scenario IIa: complete closure of the north tube (i.e., both lanes are closed due to a traffic accident) with a fire that might occur on the lane of the adjacent tube that is used by traffic traveling towards the north; Scenario IIb: similar to Scenario IIa, but with the HGVs traveling towards the north tube diverted to an alternative itinerary.

Regardless of the scenario considered, Figure 6 shows how the last escaping user is always subjected to a radiant heat flux lower than the tenability limit of 2 kW/m^2 (i.e., dotted line) [50].

5.3. Visibility Distance

Figure 7 shows the longitudinal profiles of visibility distance predicted at 2 m height along the escape path after 10 min from the start of the 100 MW (i.e., Scenarios 0, Ia, and IIa) or 15 MW (i.e., Scenarios Ib and IIb) fire located in the middle of the tunnel length. Figure 7 shows how the last escaping user always has a visibility distance greater than the tenability limit of 10 m (i.e., dotted line) [50], except for the 100 MW fire related to Scenario IIa in which he/she (the green user) might be exposed to unsafe environmental conditions due to his/her inability to discern evacuation signs located along the escape route.
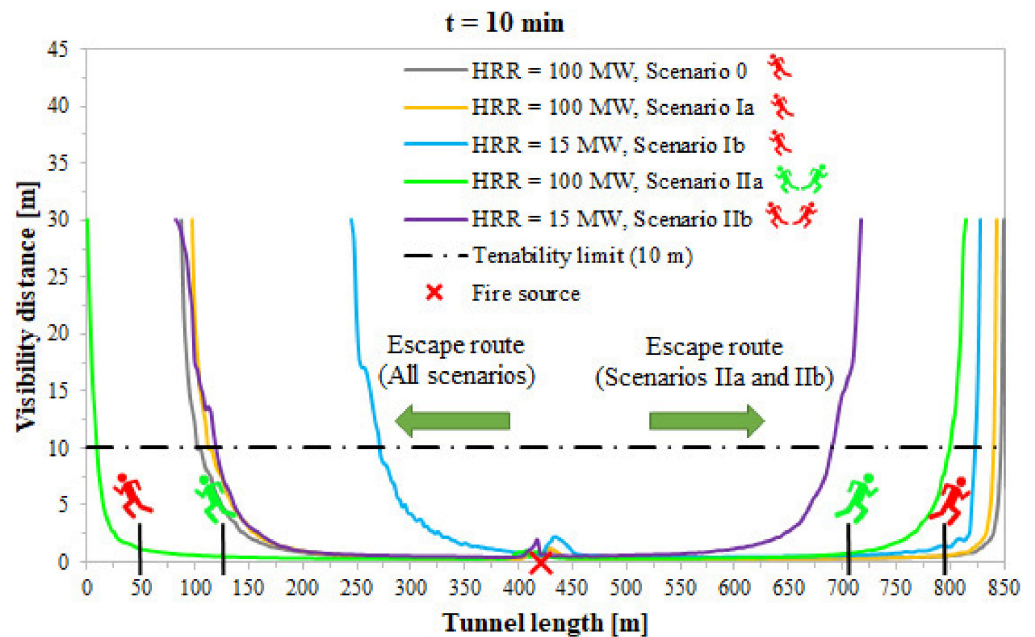
Figure 7. Longitudinal profiles of visibility distance predicted at 2 m height along the escape path after 10 min from the start of the 100 MW (i.e., Scenarios 0, Ia, and IIa) or 15 MW (i.e., Scenarios Ib and IIb) fire located in the middle of the tunnel length. Scenario 0: ordinary conditions of functionality of the tunnel system (i.e., both lanes of each tube are used for one driving direction) with a fire that occurs in the north tube; Scenario Ia: partial closure of the north tube (i.e., only the right lane is closed due to a traffic accident) with a fire that might occur on the left lane of the north tube; Scenario Ib: similar to Scenario Ia, but with the HGVs traveling towards the north tube diverted to an alternative itinerary; Scenario IIa: complete closure of the north tube (i.e., both lanes are closed due to a traffic accident) with a fire that might occur on the lane of the adjacent tube that is used by traffic traveling towards the north; Scenario IIb: similar to Scenario IIa, but with the HGVs traveling towards the north tube diverted to an alternative itinerary.

5.4. CO Concentration

Figure 8 shows the longitudinal CO concentration profiles predicted at 2 m height along the escape path after 10 min from the start of the 100 MW (i.e., Scenarios 0, Ia, and IIa) or 15 MW (i.e., Scenarios Ib and IIb) fire located in the middle of the tunnel length. Based on these profiles, the last escaping user is exposed to a CO concentration lower than the tenability limit of 1200 ppm (i.e., dotted line) [51] in Scenarios 0, Ia, Ib, and IIb, while he/she (the green user) might be exposed to unsafe environmental conditions in Scenario IIa.

5.5. CO_2 Concentration

Figure 9 shows the longitudinal profiles of CO_2 concentration predicted at 2 m height along the escape path after 10 min from the start of the 100 MW (i.e., Scenarios 0, Ia, and IIa) or 15 MW (i.e., Scenarios Ib and IIb) fire located in the middle of the tunnel length.

Figure 9 shows how the last escaping user is always exposed to a CO_2 concentration below the tenability limit of 40,000 ppm (i.e., dotted line) [51].
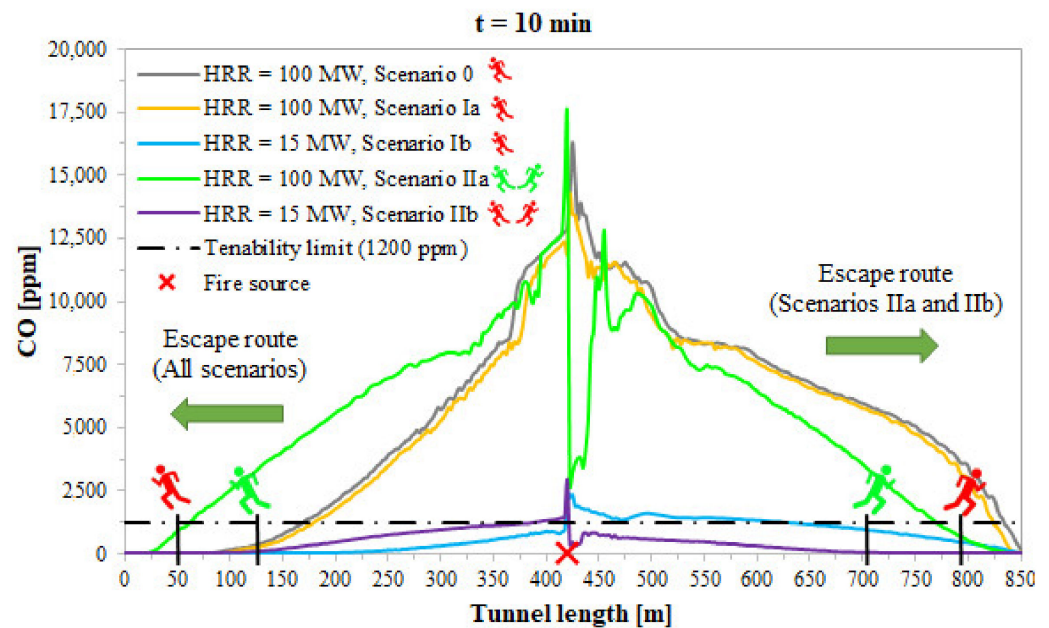
Figure 8. Profiles of longitudinal CO concentration predicted at 2 m height along the escape path after 10 min from the start of the 100 MW (i.e., Scenarios 0, Ia, and IIa) or 15 MW (i.e., Scenarios Ib and IIb) fire located in the middle of the tunnel length. Scenario 0: ordinary conditions of functionality of the tunnel system (i.e., both lanes of each tube are used for one driving direction) with a fire that occurs in the north tube; Scenario Ia: partial closure of the north tube (i.e., only the right lane is closed due to a traffic accident) with a fire that might occur on the left lane of the north tube; Scenario Ib: similar to Scenario Ia, but with the HGVs traveling towards the north tube diverted to an alternative itinerary; Scenario IIa: complete closure of the north tube (i.e., both lanes are closed due to a traffic accident) with a fire that might occur on the lane of the adjacent tube that is used by traffic traveling towards the north; Scenario IIb: similar to Scenario IIa, but with the HGVs traveling towards the north tube diverted to an alternative itinerary.

Summing up the results above, with reference to the last evacuating user: (i) better environmental conditions were observed to occur with partial closure of the tube rather than complete closure (i.e., Scenarios Ia and Ib against Scenarios IIa and IIb); (ii) additional benefits can be found by activating VMSs that suggest an alternative itinerary for HGVs only (i.e., Scenario Ib versus Scenario Ia, and Scenario IIb against Scenario IIa); this is due to the fact that when the HGVs are diverted to the alternative route, the most potentially dangerous event is represented only by a van fire (i.e., HRR_{max} of 15 MW); (iii) safety issues for human health may arise only in the event of 100 MW fire occurring during the complete closure of the north tube and the use of the parallel one for two-way traffic (i.e., Scenario IIa) due to exceeding the acceptable limit of 10 m and 1200 ppm for the visibility distance and CO concentration, respectively.

It is worth highlighting that similar evacuation conditions were also found for the remaining locations of the burning vehicle (i.e., 145, 280, 570, 710 m from portal A of the north tube for Scenarios 0, Ia, and Ib, or from portal D of the adjacent tube used for bi-directional traffic for Scenarios IIa and IIb). With reference to the remaining HRR_{max} investigated (i.e., 8, 15, 30, and 50 MW fires for Scenarios 0, Ia, and IIa; or 8 MW fire for Scenarios Ib and IIb) and locations of the fire in the tunnel tube, we did not find any unsafe conditions for the users evacuating the tube. However, it needs to be stressed that, in order to save space, in the present paper, we have reported only the results of the worst-case scenarios that were found to be the burning vehicles with HRR_{max} = 100 MW located in the middle of the tunnel tube length for Scenarios 0, Ia, and IIa, and for the fire of 15 MW in Scenarios Ib and IIb.
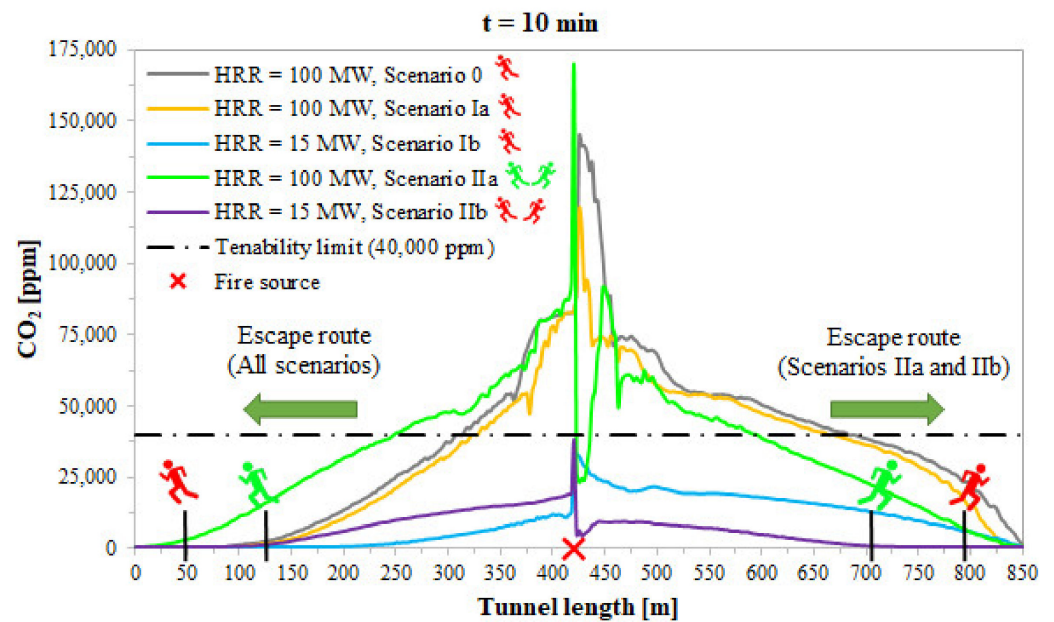
Figure 9. Longitudinal CO_2 concentration profiles predicted at 2 m height along the escape path after 10 min from the start of the 100 MW (i.e., Scenarios 0, Ia, and IIa) or 15 MW (i.e., Scenarios Ib and IIb) fire located in the middle of the tunnel length. Scenario 0: ordinary conditions of functionality of the tunnel system (i.e., both lanes of each tube are used for one driving direction) with a fire that occurs in the north tube; Scenario Ia: partial closure of the north tube (i.e., only the right lane is closed due to a traffic accident) with a fire that might occur on the left lane of the north tube; Scenario Ib: similar to Scenario Ia, but with the HGVs traveling towards the north tube diverted to an alternative itinerary; Scenario IIa: complete closure of the north tube (i.e., both lanes are closed due to a traffic accident) with a fire that might occur on the lane of the adjacent tube that is used by traffic traveling towards the north; Scenario IIb: similar to Scenario IIa, but with the HGVs traveling towards the north tube diverted to an alternative itinerary.

5.6. Back-Layering Phenomenon and Smoke Stratification

Figure 10 shows the back-layering phenomenon and smoke stratification predicted along the escape route after 10 min from the start of the fire of 100 MW (i.e., Scenarios 0, Ia, and IIa) or 15 MW (i.e., Scenarios Ib and IIb) located in the middle of the tunnel length. It shows that the last escaping user is always exposed to safe evacuation conditions, except for the 100 MW fire of Scenario IIa in which the aforementioned user (i.e., the green user) might be a victim of serious risks to human health due to smoke spread. Figure 10 shows that: (i) the natural ventilation due to the piston effect of moving vehicles is not able to prevent the back-layering phenomenon (i.e., the smoke propagation in the opposite direction of the natural ventilation); (ii) with increase in HRR_{max} (i.e., the 100 MW for Scenario Ia in contrast to the 15 MW for Scenario Ib, and the 100 MW for Scenario IIa versus the 15 MW for Scenario IIb), worse smoke conditions are found on the left sidewalk of the north tube and both sidewalks of the parallel tube used for two-way traffic, respectively; (iii) the smoke layering length is not symmetrical for Scenarios 0, Ia, and Ib due to the natural ventilation that pushes the smoke towards portal B (i.e., pressure difference of 5 Pa from portal A to portal B); (iv) the smoke distribution in the adjacent tube (i.e., Scenarios IIa and IIb) is almost symmetrical in the two directions upstream and downstream of the fire because of the reduced pressure difference between the tunnel portals (i.e., 0.5 Pa from portal C to portal D, or equivalently −0.5 Pa from portal D to portal C, that very slowly pushes the air flow towards portal D).
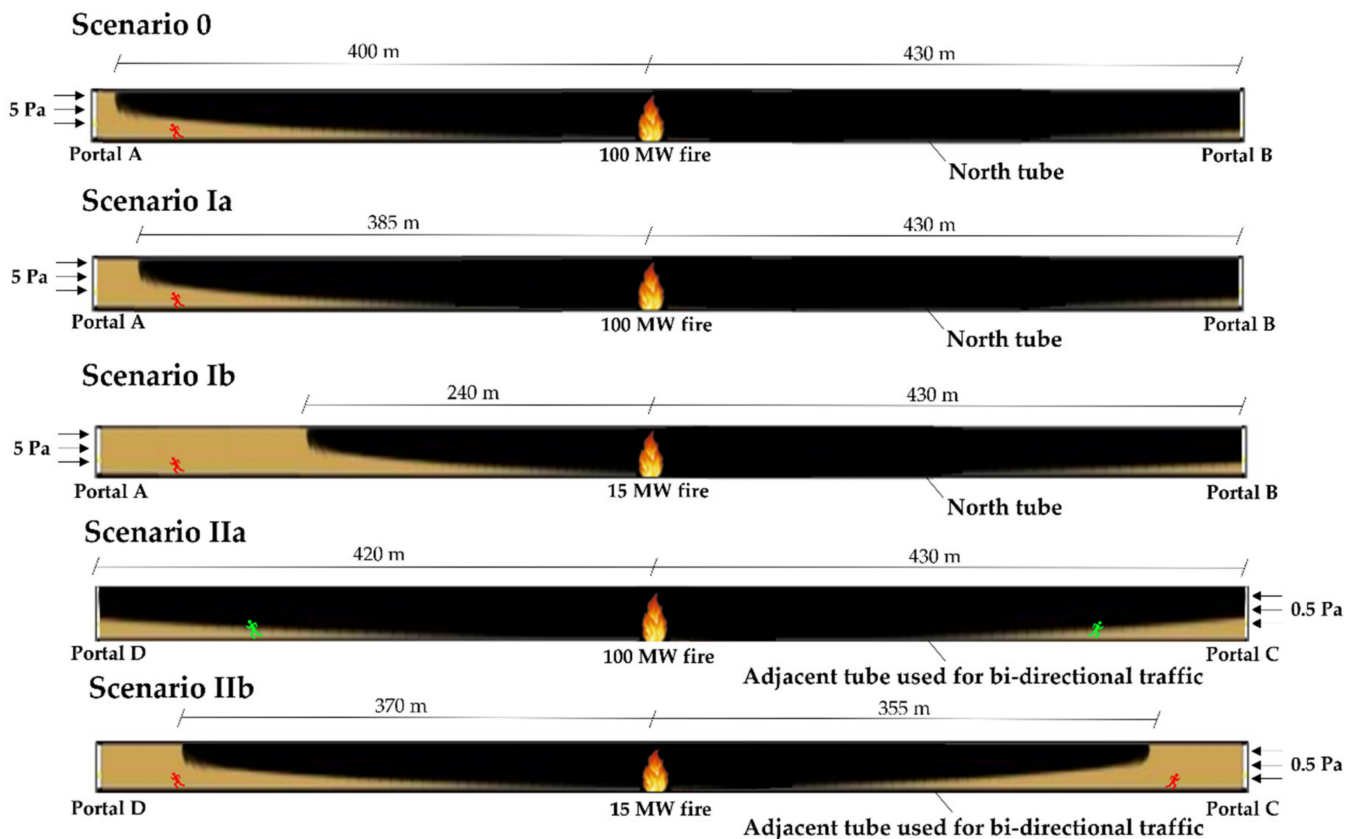
Figure 10. Contours of smoke propagation predicted along the escape route after 10 min from the start of the fire of 100 MW (i.e., Scenarios 0, Ia, and IIa with HGVs) or 15 MW (i.e., Scenarios Ib and IIb without HGVs) located in the middle of the tunnel length. Scenario 0: ordinary conditions of functionality of the tunnel system (i.e., both lanes of each tube are used for one driving direction) with a fire that occurs in the north tube; Scenario Ia: partial closure of the north tube (i.e., only the right lane is closed due to a traffic accident) with a fire that might occur on the left lane of the north tube; Scenario Ib: similar to Scenario Ia, but with the HGVs traveling towards the north tube diverted to an alternative itinerary; Scenario IIa: complete closure of the north tube (i.e., both lanes are closed due to a traffic accident) with a fire that might occur in the lane of the adjacent tube that is used by traffic traveling towards the north; Scenario IIb: similar to Scenario IIa, but with the HGVs traveling towards the north tube diverted to an alternative itinerary.

Therefore, Figure 10 also confirms, with respect to smoke layering, that better environmental conditions are found with the partial closure of the tube rather than complete closure, and that additional advantages can be found through the activation of VMSs that suggest an alternative route for HGVs only.

6. Quantitative Risk Analysis

6.1. Methodological Approach

A quantitative risk analysis (QRA) based on a probabilistic approach was carried out to estimate the consequences in terms of the number of potential victims associated with the scenarios simulated by means of the FDS + Evac modeling. The main steps for implementing a probabilistic approach, which involves an event tree, fault tree, and models for estimating the consequences, entail the choice of objective, specification of the tunnel, classification of each hazard and evaluation of its probability (or frequency) of occurrence, evaluation of the consequences on user health, estimation of the risk as the sum of the probabilities multiplied by the consequences, choice of the risk acceptability criterion, and quantification of the risk level.

The so-called societal risk is generally the main outcome of a QRA and is commonly expressed graphically in terms of F-N curves (F is the annual cumulative frequency of potential fatalities N) or numerically in terms of the expected value (EV) of risk (EV = $\int_1^{+\infty}$ F(N)dN). The aforementioned F-N curves might be used to compare the risk level of a given tunnel under different scenarios and/or with the unacceptable and acceptable risk limits of the ALARP (As Low As Reasonably Practicable) region.

6.2. Event Tree

The identification of each hazard (i.e., fires characterized by an HRR_{max} of 8, 15, 30, 50, or 100 MW) and the estimation of its probability of occurrence are made using the event tree. It should be noted that the event tree is designed in a graphic form to depict several chronological series of successive events starting from an initial event. Specifically, it reports the probability (p) of the occurrence of each intermediate event based on the probability of the initial event. In this paper, we used the event tree proposed by ANAS [52]. The initial event consists of the annual frequency of traffic accidents in road tunnels, which is followed by: traffic collisions (p = 94.9%) and fires (p = 5 %). Fires might involve light vehicles (p = 70%) or heavy vehicles (p = 30%) and are classified as relevant (p = 70% for light vehicles, or p = 20% for heavy vehicles) or non-relevant (p = 30% for light vehicles, or p = 80% for heavy vehicles). The relevant fires involving light vehicles might entail an HRR_{max} of 8 MW (p = 2.5%), while those involving heavy vehicles might be characterized by an HRR_{max} of 15, 30, 50, and 100 MW (p = 81.5, 14.5, 2.5, and 1.5%, respectively).

6.3. Annual Frequency of Traffic Accidents

To estimate the annual frequency of traffic accidents, which represents the initial event in the event tree, the average accident rate (i.e., the average number of accidents per 100 million vehicle-kilometers) of 43.5 accidents/10^8 vehicle-km provided by the tunnel management agency (TMA) for the investigated tunnel was considered. It is worth noting that the risk analysis was carried out considering the partial or complete closure of the north tube for three hours due to the occurrence of a traffic accident on the right lane of this tube, since this was the worst-case scenario in our previous study on tunnel resilience.

Therefore, by considering the three hours of peak-traffic volumes (see Section 2.3), we computed the corresponding equivalent annual average daily traffic (EAADT) for each scenario investigated: 6600 vehicles/day (i.e., 2200 vehicles/h for the two unidirectional lanes) for Scenario 0; 5100 vehicles/day (i.e., 1700 vehicles/h for one lane) for Scenarios Ia and Ib; and 9600 vehicles/day (i.e., 3200 vehicles/h for the two bi-directional lanes) for Scenarios IIa and IIb.

Based on the EAADTs and accident rate, the annual frequency of traffic accidents (i.e., the average number of accidents per year) was found to be: 0.891 for Scenario 0; 0.688 for Scenarios Ia and Ib; and 1.3 for Scenarios IIa and IIb. These values were implemented as the initial event in the event tree.

6.4. Annual Fire Frequency

The annual frequency of each fire scenario reproduced through the FDS + Evac codes was estimated as the product of the annual frequency of traffic accidents and the probabilities of all the intermediate events included between the initial and final events in the event tree (e.g., with reference to the 100 MW fire for Scenario IIa, we calculated this as: $1.3 \times 0.05 \times 0.3 \times 0.2 \times 0.015 = 5.85 \times 10^{-5}$). Table 2 reports the annual frequency of occurrence of each scenario investigated.

Table 2. Annual frequency of occurrence of each scenario reproduced through the FDS + Evac codes. Scenario 0: ordinary conditions of functionality of the tunnel system (i.e., both lanes of each tube are used for one driving direction) with a fire that occurs in the north tube; Scenario Ia: partial closure of the north tube (i.e., only the right lane is closed due to a traffic accident) with a fire that might occur on the left lane of the north tube; Scenario Ib: similar to Scenario Ia, but with the HGVs traveling towards the north tube diverted to an alternative itinerary; Scenario IIa: complete closure of the north tube (i.e., both lanes are closed due to a traffic accident) with a fire that might occur on the lane of the adjacent tube that is used by traffic traveling towards the north; Scenario IIb: similar to Scenario IIa, but with the HGVs traveling towards the north tube diverted to an alternative itinerary.

Scenario	Annual Frequency of Occurrence of Fire Scenarios [1/Year]				
	8 MW	**15 MW**	**30 MW**	**50 MW**	**100 MW**
0	4.46×10^{-4}	2.18×10^{-3}	3.88×10^{-4}	6.68×10^{-5}	4.01×10^{-5}
Ia	4.22×10^{-4}	1.68×10^{-3}	2.99×10^{-4}	5.16×10^{-5}	3.10×10^{-5}
Ib	4.22×10^{-4}	1.68×10^{-3}	-	-	-
IIa	7.96×10^{-4}	3.18×10^{-3}	5.66×10^{-4}	9.75×10^{-5}	5.85×10^{-5}
IIb	7.96×10^{-4}	3.18×10^{-3}	-	-	-

Moreover, each of the five positions at which the burning vehicle was assumed to be located along the tunnel length (i.e., 145, 280, 420, 570, and 710 m from portal A of the north tube for Scenarios 0, Ia, and Ib, or portal D of the parallel tube used for two-way traffic for Scenarios IIa and IIb) was given the same probability of occurrence, thus equal to 0.2. Consequently, the values reported in Table 2 were multiplied by 0.2 to estimate the annual frequency of occurrence of a certain fire in each mentioned location of the burning vehicle in the tunnel.

6.5. F-N Curves

In this paper, the fractional effective dose (FED) was used to calculate the number of people at risk in the event of a fire in the tunnel tube investigated. Based on the FED concept, an evacuee is considered as a potential victim when the FED corresponding to his/her exposure to temperatures and radiant heat fluxes (FED_{heat}) and/or toxic substances ($FED_{toxic\ gases}$) exceeds unity (for more details see Caliendo et al. [29]). It should be noted that the QRA was performed by considering the FED of all the evacuees and their entire egress process from the tunnel, which occurs using: (i) both the right and left sidewalk upstream of the burning vehicle for Scenario 0 (i.e., users escaping towards portal A); (ii) the left sidewalk upstream of the fire source for Scenarios Ia and Ib (i.e. users escaping towards portal A); (iii) the right sidewalk upstream of the fire for the users escaping towards portal D, and the right sidewalk downstream of the fire for the users escaping towards portal C for Scenarios IIa and IIb.

This was carried out for each HRR_{max} (i.e., 8, 15, 30, 50, and 100 MW for Scenarios 0, Ia, and IIa, and 8 and 15 MW for Scenarios Ib and IIb) and location (i.e., 145, 280, 420, 570, and 710 m from portal A of the north tube for Scenarios 0, Ia, and Ib, or portal D of the adjacent tube for Scenarios IIa and IIb) of the fire. For some of the combinations of HRR_{max} and location of the burning vehicle, the $FED_{toxic\ gases}$ was computed to be greater than 1, while the FED_{heat} was always found to be much less than 1. As a result, the estimated number of people at risk derives only from their exposure to toxic gases.

Then, the number of potential victims, referred to each HRR_{max} and location of the fire, was associated with the corresponding annual frequency of fire occurrence in order to compute the individual cumulative frequency of each fire. Subsequently, by combining the individual cumulative frequencies, we calculated the final cumulative frequency with respect to the escaping users from one of the tunnel portals and/or the emergency exit.

Figure 11 shows, in a bi-logarithmic diagram, the F-N curves for each scenario investigated, as well as the unacceptable and acceptable limits of the Italian ALARP region.
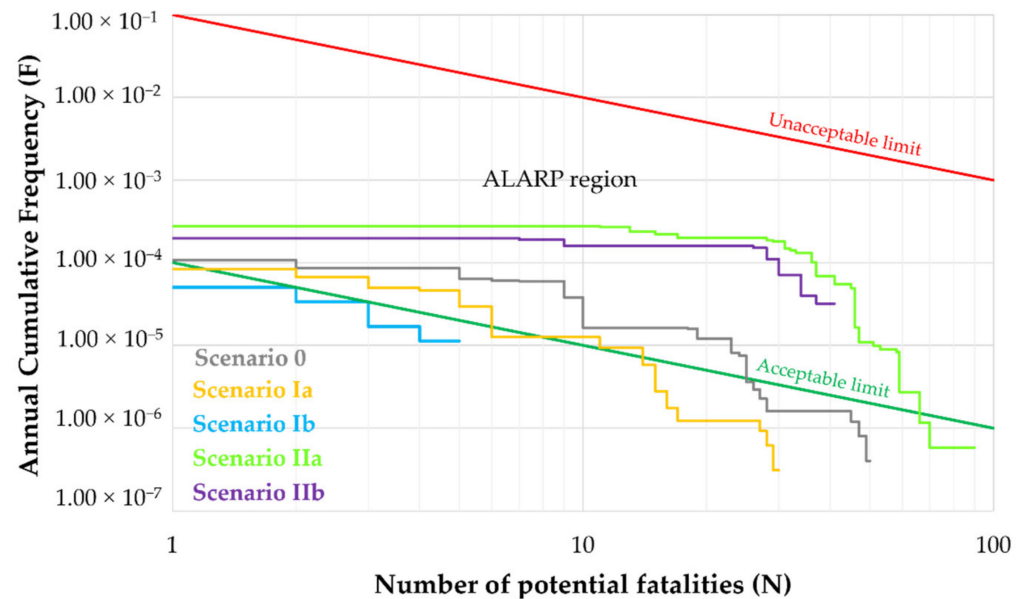
Figure 11. F-N curves for each scenario investigated. Scenario 0: ordinary conditions of functionality of the tunnel system (i.e., both lanes of each tube are used for one driving direction) with a fire that occurs in the north tube; Scenario Ia: partial closure of the north tube (i.e., only the right lane is closed due to a traffic accident) with a fire that might occur on the left lane of the north tube; Scenario Ib: similar to Scenario Ia, but with the HGVs traveling towards the north tube diverted to an alternative itinerary; Scenario IIa: complete closure of the north tube (i.e., both lanes are closed due to a traffic accident) with a fire that might occur on the lane of the adjacent tube that is used by traffic traveling towards the north; Scenario IIb: similar to Scenario IIa, but with the HGVs traveling towards the north tube diverted to an alternative itinerary.

Figure 11 shows how all the F-N curves lie below the unacceptable limit of the ALARP region. The partial closure of the north tube presents a lower risk level than that associated with the tunnel in its ordinary conditions of functionality (i.e., Scenarios Ia and Ib against Scenario 0). This is because Scenarios Ia and Ib are characterized by a lower traffic volume (1700 vehicles/h for Scenarios Ia and Ib against 2200 vehicles/h for Scenario 0) and consequently by a lower number of users exposed to risk (only one lane is available to traffic before the start of the fire) than Scenario 0. In contrast, the F-N curves corresponding to the scenarios involving the complete closure of the north tube and the use of the parallel one for two-way traffic (i.e., Scenarios IIa and IIb) always lie above that of Scenario 0. This might be explained by the higher traffic volume (3200 vehicles/h for Scenarios IIa and IIb against 2200 vehicles/h for Scenario 0) and thus the greater number of potential victims expected in the adjacent tube when it is employed for two-way traffic.

Figure 11 also shows that, both in the case of the partial and of the complete closure of the north tube, certain benefits in terms of users' safety, might be found by activating VMSs, situated at a reasonable distance from the motorway junction before the entrance portal of the north tube, for diverting only HGVs towards an alternative itinerary (i.e., Scenario Ib versus Scenario Ia, and Scenario IIb against Scenario IIa). These benefits are because the fires, involving only cars and vans traveling towards the north, are characterized by a reduced HRR_{max} compared to those of HGVs. Moreover, Scenario Ib (i.e., partial closure of the north tube with HGVs redirected to the alternative itinerary) presents the lowest level of risk among the scenarios investigated.

6.6. Resilience Index and Expected Value of Risk for Each Scenario

Figure 12 summarizes the results of the simultaneous analysis of user safety and resilience reported in Caliendo et al. [25] for each scenario investigated expressed in terms of the expected value (EV) of risk and resilience index, respectively. It should be noted that the EV of risk represents the area subtended by the F-N curve (i.e., $EV = \int_1^{+\infty} F(N)dN$).
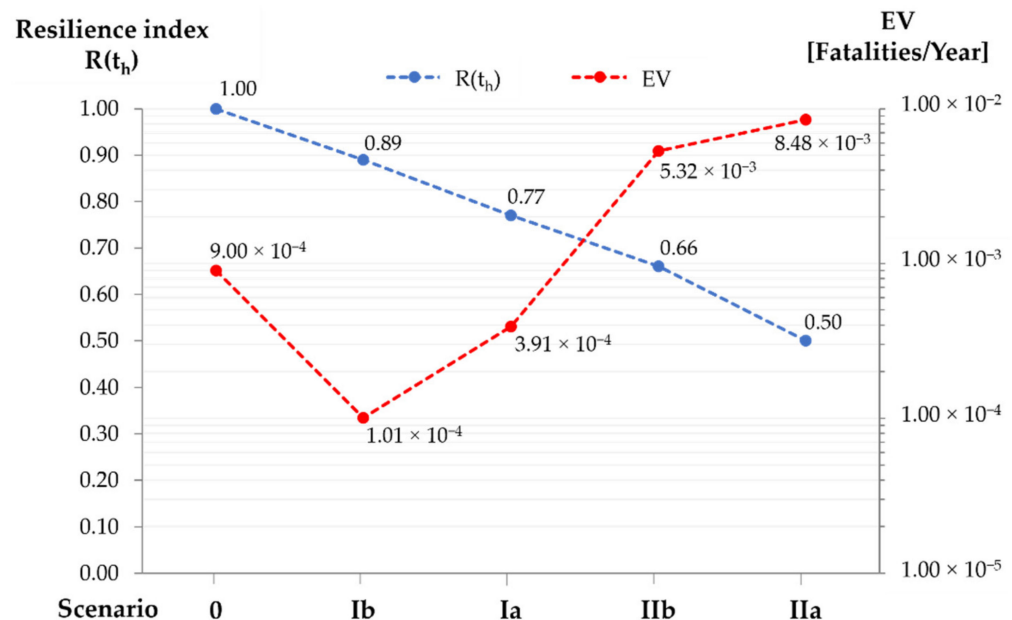

Figure 12. Resilience index and expected value (EV) of risk for each scenario investigated. Scenario 0: ordinary conditions of functionality of the tunnel system (i.e., both lanes of each tube are used for one driving direction) with a fire that occurs in the north tube; Scenario Ia: partial closure of the north tube (i.e., only the right lane is closed due to a traffic accident) with a fire that might occur on the left lane of the north tube; Scenario Ib: similar to Scenario Ia, but with the HGVs traveling towards the north tube diverted to an alternative itinerary; Scenario IIa: complete closure of the north tube (i.e., both lanes are closed due to a traffic accident) with a fire that might occur on the lane of the adjacent tube that is used by traffic traveling towards the north; Scenario IIb: similar to Scenario IIa, but with the HGVs traveling towards the north tube diverted to an alternative itinerary.

Figure 12 shows how the lowest value of risk, expressed by the EV of risk, is found in the case of the partial closure of the north tube when the alternative itinerary is activated for HGVs only (i.e., Scenario Ib), and that the associated resilience index is only a little lower than 1 (i.e., 0.89), which indicates a small resilience loss. The EV of risk increases when the north tube is partially closed with its left lane used by all the vehicles, while the corresponding resilience index decreases from 0.89 to 0.77 (i.e., Scenario Ia presents a slightly higher resilience loss than Scenario Ib). However, in both cases, the value of the EV of risk is less than that corresponding to the ordinary conditions of functionality of the north tube (i.e., Scenario 0).

In contrast, with reference to the complete closure of the north tube, the values of EV of risk are found to be higher than that of Scenario 0, and the resilience index decreases up to 0.66 and 0.50 for Scenarios IIb and IIa, respectively, which indicates a more significant resilience loss.

7. Summary and Conclusions

The present study was mainly motivated by the need to simultaneously couple user safety with resilience in order to identify the most appropriate arrangement to be adopted in the event of a traffic accident in a tube of a twin-tube road tunnel. In this respect, we investigated different scenarios by assuming that during the partial or complete closure of

a tube, because of the occurrence of a traffic accident, a fire might simultaneously occur on the undisrupted remaining lane, or in the parallel tube used for two-way traffic in the case of the partial or complete closure of the disrupted tube, respectively.

For this purpose, we developed a computational fluid dynamics (CFD) model, and simulated the corresponding egress process, to evaluate the risk level of tunnel users in the event of a fire. The Fire Dynamics Simulator (FDS) code, as well as its evacuation module (Evac), were implemented, and their output were used to carry out a quantitative risk analysis (QRA) based on a probabilistic approach.

The effects of five different types of burning vehicles were investigated. Each burning vehicle was assumed to be located at five different positions along the remaining undisrupted lane, or in the parallel tube used for two-way traffic in the case of the partial or complete closure of the tube affected by the traffic accident. The burning vehicles were assumed to be two cars, a van, a bus, and two different types of HGVs capable of developing a maximum heat release rate (HRR_{max}) of 8, 15, 30, 50, and 100 MW, respectively.

With reference to the last user escaping from the tunnel tube in the event of a fire, the findings of the CFD simulations, in terms of temperature, radiant heat flux, visibility distance, and toxic gases concentration at breathing height along the escape route, showed that: (i) better environmental conditions were found with partial closure of the tube rather than complete closure; (ii) additional benefits can be found by activating variable message signs (VMSs) that suggest an alternative itinerary for HGVs only; (iii) safety issues for human health may arise only in the case of a 100 MW fire, occurring during the complete closure of the north tube and the use of the parallel one for bi-directional traffic, due to exceeding the acceptable tenability limits of both visibility distance and CO concentration.

The results of the QRA were found to be consistent with those obtained by CFD modeling, as follows: (i) the partial closure of the tube presents a lower risk level than that associated with the tube in its ordinary conditions of functionality; (ii) the complete closure of a tube and the use of the parallel tube for two-way traffic leads to a higher risk level compared to that of the ordinary conditions of functionality of the tunnel; (iii) additional reductions in risk can be found by activating VMSs to divert only HGVs towards an alternative itinerary.

The lowest value of risk (expressed by the expected value (EV) of risk), which corresponded to the case of the partial closure of the north tube and the activation of an alternative route for HGVs only, was found to be associated with a resilience index slightly less than one, which showed a small resilience loss. The EV of risk increases when the north tube is partially closed with its left lane used by all the vehicles, and the corresponding resilience index was found to be slightly decreased. However, in both cases the value of the EV is less than that corresponding to the ordinary conditions of functionality of the tunnel tube. In contrast, with reference to the complete closure of the north tube, the values of the EV of risk were found to be higher than that of the tunnel in its ordinary conditions of functionality, while the resilience index decreased, which indicated a more significant resilience loss.

The scientific significance of the present paper lies in increasing our knowledge in the research area of both fire safety engineering and tunnel management, and in the dissemination of additional information for the operating conditions of tunnels.

This study provides valuable perspectives on both relevant aspects of user safety and the resilience of road tunnels at the same time. It can serve as a possible reference for tunnel management agencies (TMAs) in the choice of the most appropriate strategy for the recovery process of system functionality in the event of an incident.

Although the present paper represents an advancement in the context of research on the simultaneous analysis of user safety and tunnel resilience, the randomness of certain parameters might create some uncertainties. Moreover, disruption in a road tunnel might also propagate to other transport systems. Our modeling is likely to be generally valid for tunnels having a length ≤ 1 km, which are by far the most frequent in Italy. However, additional studies should also involve much longer tunnels which use innovative

equipment that may be automatically activated when a fire starts, as an alternative or supplementary measure to hydrants, in order to contrast fire growth phases in road tunnels.

Therefore, further studies, based on analysis of uncertainties and intermodal transport, need to be completed.

Author Contributions: Conceptualization, C.C., G.G. and I.R.; methodology, C.C., G.G. and I.R.; software, C.C., G.G. and I.R.; validation, C.C., G.G. and I.R.; formal analysis, C.C., G.G. and I.R.; investigation, C.C., G.G. and I.R.; data curation, C.C., G.G. and I.R.; writing—original draft preparation, C.C., G.G. and I.R.; writing—review and editing, C.C., G.G. and I.R.; visualization, C.C., G.G. and I.R.; supervision, C.C. All authors have read and agreed to the published version of the manuscript.

Institutional Review Board Statement: Not applicable.

Informed Consent Statement: Informed consent was obtained from all the subjects involved in the study.

Data Availability Statement: The data presented in this study are available upon request from the corresponding author. The data are not publicly available due to privacy restrictions.

Conflicts of Interest: The authors declare no conflict of interest.

Nomenclature

Symbol	Unit	Description
ALARP		As Low As Reasonably Practicable
CFD		Computational fluid dynamics
CO		Carbon monoxide
EAADT	vehicles/day	Equivalent annual average daily traffic
EV of risk	fatalities/year	Expected value of risk
F	1/year	Annual cumulative frequency
F*	%	Functionality
FDS		Fire Dynamics Simulator
FED		Fractional effective dose
HGV		Heavy goods vehicle
HRR	MW	Heat release rate
N		Number of potential fatalities
p	%	Probability
QRA		Quantitative risk analysis
t	min	Time
TMA		Tunnel management agency
VHP	vehicles/h	Hourly traffic volume
VMS		Variable message sign
Sup and subscripts		
CO_2		Carbon dioxide
FED_{heat}		Fractional effective dose due to heat exposure
$FED_{toxic\ gases}$		Fractional effective dose due to toxic gases exposure
HRR_{max}	MW	Maximum heat release rate
t_h	min	Time when the tunnel system is fully functional
t_{max}	min	Time to reach the maximum HRR
t_o	min	Time when the traffic accident occurs

References

1. Caliendo, C.; Guida, M.; Parisi, A. A crash-prediction model for multilane roads. *Accid. Anal. Prev.* **2007**, *39*, 657–670. [CrossRef] [PubMed]
2. Caliendo, C.; De Guglielmo, M.L.; Guida, M. A crash-prediction model for road tunnels. *Accid. Anal. Prev.* **2013**, *55*, 107–115. [CrossRef] [PubMed]
3. Caliendo, C.; Guida, M. A new bivariate regression model for the simultaneous analysis of total and severe crashes occurrence. *J. Transp. Saf. Secur.* **2014**, *6*, 78–92. [CrossRef]

4. Caliendo, C.; De Guglielmo, M.L.; Guida, M. Comparison and analysis of road tunnel traffic accident frequencies and rates using random-parameter model. *J. Transp. Saf. Secur.* **2016**, *8*, 177–195. [CrossRef]

5. Caliendo, C.; De Guglielmo, M.L.; Russo, I. Analysis of crash frequency in motorway tunnels based on a correlated random-parameters approach. *Tunn. Undergr. Space Technol.* **2019**, *85*, 243–251. [CrossRef]

6. Caliendo, C.; Guida, M.; Postiglione, F.; Russo, I. A Bayesian bivariate hierarchical model with correlated parameters for the analysis of road crashes in Italian tunnels. *Stat. Methods. Appl.* **2022**, *31*, 109–131. [CrossRef]

7. Freckleton, D.; Heaslip, K.; Louisell, W.; Collura, J. Evaluation of Resiliency of Transportation Networks after Disasters. *Transp. Res. Rec.* **2012**, *2284*, 109–116. [CrossRef]

8. Faturechi, R.; Miller-Hooks, E. Measuring the Performance of Transportation Infrastructure Systems in Disasters: A Comprehensive Review. *J. Infrastruct. Syst.* **2015**, *21*, 04014025. [CrossRef]

9. D'Lima, M.; Medda, F. A new measure of resilience: An application to the London Underground. *Transp. Res. A Policy Pract.* **2015**, *81*, 35–46. [CrossRef]

10. Sun, W.; Bocchini, P.; Davison, B.D. Resilience metrics and measurement methods for transportation infrastructure: The state of the art. *Sustain. Resilient Infrastruct.* **2020**, *5*, 168–199. [CrossRef]

11. Knoop, V.; van Zuylen, H.; Hoogendoorn, S. The influence of spillback modelling when assessing consequences of Blockings in a road network. *Eur. J. Transp. Infrastruct. Res.* **2008**, *8*, 287–300. [CrossRef]

12. Liao, S.Y.; Hu, T.Y.; Ho, W.M. Simulation studies of traffic management strategies for a long tunnel. *Tunn. Undergr. Sp. Technol.* **2012**, *27*, 123–132. [CrossRef]

13. Omer, M.; Mostashari, A.; Nilchiani, R. Measuring the resiliency of the Manhattan points of entry in the face of severe disruption. *Am. J. Eng. Appl. Sci.* **2011**, *4*, 153–161. [CrossRef]

14. Antoniou, C.; Koutsopoulos, H.N.; Ben-Akiva, M.; Chauhan, A.S. Evaluation of diversion strategies using dynamic traffic assignment. *Transp. Plan. Technol.* **2011**, *34*, 199–216. [CrossRef]

15. Reggiani, A.; Nijkamp, P.; Lanzi, D. Transport resilience and vulnerability: The role of connectivity. *Transp. Res. A Policy Pract.* **2015**, *81*, 4–15. [CrossRef]

16. Kaviani, A.; Thompson, R.G.; Rajabifard, A. Improving regional road network resilience by optimised traffic guidance. *Transp. A Transp. Sci.* **2017**, *13*, 794–828. [CrossRef]

17. Amini, S.; Tilg, G.; Busch, F. Evaluating the impact of real-time traffic control measures on the resilience of urban road networks. In Proceedings of the 21st International Conference on Intelligent Transportation Systems (ITSC), Maui, HI, USA, 4–7 November 2018; pp. 519–524. [CrossRef]

18. Xu, X.; Chen, A.; Jansuwan, S.; Chao Yang, C.; Ryu, S. Transportation network redundancy: Complementary measures and computational methods. *Transp. Res. B Methodol.* **2018**, *114*, 68–85. [CrossRef]

19. Sohouenou, P.Y.R.; Neves, L.A.C. Assessing the effects of link-repair sequences on road network resilience. *Int. J. Crit. Infrastruct. Prot.* **2021**, *34*, 100448. [CrossRef]

20. Abudayyeh, D.; Nicholson, A.; Ngoduy, D. Traffic signal optimisation in disrupted networks, to improve resilience and sustainability. *Travel Behav. Soc.* **2021**, *22*, 117–128. [CrossRef]

21. Khetwal, S.S.; Pei, S.; Gutierrez, M. Stochastic event simulation model for quantitative prediction of road tunnel downtime. *Tunn. Undergr. Sp. Technol.* **2021**, *116*, 104092. [CrossRef]

22. Zhao, F. Research on resilience recovery strategy optimization of highway after disaster based on genetic algorithm. *J. Phys. Conf. Ser.* **2021**, *2083*, 032014. [CrossRef]

23. PIARC. *PIARC Literature Review—Improving Road Tunnel Resilience, Considering Safety and Availability*; Technical Committee on Road Tunnels, The World Road Association: Paris, France, 2021. Available online: https://www.piarc.org/en/order-library/35017-en-ImprovingRoad%20Tunnel%20Resilience,%20Considering%20Safety%20and%20Availability%20-%20PIARC%20Literature%20Review (accessed on 2 February 2022).

24. Borghetti, F.; Frassoldati, A.; Derudi, M.; Lai, I.; Trinchini, C. Resilience and Emergency Management of Road Tunnels: The Case Study of the San Rocco and Stonio Tunnels in Italy. *Saf. Secur. Eng. IX* **2021**, *1*, 81–92. [CrossRef]

25. Caliendo, C.; Russo, I.; Genovese, G. Resilience Assessment of a Twin-Tube Motorway Tunnel in the Event of a Traffic Accident or Fire in a Tube. *Appl. Sci.* **2022**, *12*, 513. [CrossRef]

26. Caliendo, C.; Ciambelli, P.; De Guglielmo, M.L.; Meo, M.G.; Russo, P. Numerical simulation of different HGV fire scenarios in curved bi-directional road tunnels and safety evaluation. *Tunn. Undergr. Sp. Technol.* **2012**, *31*, 33–50. [CrossRef]

27. Caliendo, C.; Ciambelli, P.; De Guglielmo, M.L.; Meo, M.G.; Russo, P. Simulation of fire scenarios due to different vehicle types with and without traffic in a bi-directional road tunnel. *Tunn. Undergr. Sp. Technol.* **2013**, *37*, 22–36. [CrossRef]

28. Caliendo, C.; Ciambelli, P.; De Guglielmo, M.L.; Meo, M.G.; Russo, P. Computational analysis of fire and people evacuation for different positions of burning vehicles in a road tunnel with emergency exits. *Cogent Eng.* **2018**, *5*, 1–27. [CrossRef]

29. Caliendo, C.; Ciambelli, P.; Del Regno, R.; Meo, M.G.; Russo, P. Modeling and numerical simulation of pedestrian flow evacuation from a multi-storey historical building in the event of fire applying safety engineering tools. *J. Cult. Herit.* **2020**, *41*, 188–199. [CrossRef]

30. Caliendo, C.; Genovese, G.; Russo, I. Risk analysis of road tunnels: A computational fluid dynamic model for assessing the effects of natural ventilation. *Appl. Sci.* **2021**, *11*, 32. [CrossRef]

31. Caliendo, C.; Russo, I.; Genovese, G. Risk analysis of one-way road tunnel tube used for bi-directional traffic under fire scenarios. *Appl. Sci.* **2021**, *11*, 3198. [CrossRef]
32. Caliendo, C.; Genovese, G.; Russo, I. A Numerical Study for Assessing the Risk Reduction Using an Emergency Vehicle Equipped with a Micronized Water System for Contrasting the Fire Growth Phase in Road Tunnels. *Appl. Sci.* **2021**, *11*, 5248. [CrossRef]
33. Caliendo, C.; De Guglielmo, M.L. Quantitative risk analysis on the transport of dangerous goods through a bi-directional road tunnel. *Risk Anal.* **2017**, *37*, 116–129. [CrossRef] [PubMed]
34. Caliendo, C.; De Guglielmo, M.L. Quantitative risk analysis based on the impact of traffic flow in a road tunnel. *Int. J. Math. Comput. Simul.* **2016**, *10*, 39–45.
35. Caliendo, C.; Guglielmo, M.L. Simplified method for risk evaluation in unidirectional road tunnels related to dangerous goods vehicles. *Int. J. Civil. Eng. Technol.* **2017**, *8*, 960–968.
36. Caliendo, C.; De Guglielmo, M.L. Risk level evaluation of dangerous goods through road tunnels. In *Pavement and Asset Management, Proceedings of the World Conference on Pavement and Asset Management, Baveno, Italy, 12–16 June 2017*; CRC Press: London, UK, 2019; pp. 779–786.
37. Caliendo, C.; Genovese, G. Quantitative Risk Assessment on the Transport of Dangerous Goods Vehicles Through Unidirectional Road Tunnels: An Evaluation of the Risk of Transporting Hydrogen. *Risk Anal.* **2021**, *41*, 1522–1539. [CrossRef]
38. National Research Council. *HCM 2010: Highway Capacity Manual*; Transportation Research Board: Washington, DC, USA, 2010; Volume 2, ISBN 9788578110796.
39. Schrefler, B.A.; Brunello, P.; Gawin, D.; Majorana, C.E.; Pesavento, F. Concrete at high temperature with application to tunnel fire. *Comput. Mech.* **2002**, *29*, 43–51. [CrossRef]
40. Caliendo, C.; Guida, M. Microsimulation Approach for Predicting Crashes at Unsignalized Intersections Using Traffic Conflicts. *J. Transp. Eng.* **2012**, *138*, 1453–1467. [CrossRef]
41. Caliendo, C.; De Guglielmo, M.L. Road Transition Zones between the Rural and Urban Environment: Evaluation of Speed and Traffic Performance Using a Microsimulation Approach. *J. Transp. Eng.* **2013**, *139*, 295–305. [CrossRef]
42. Caliendo, C.; Parisi, A. A Stress-prediction model for airport pavements with jointed concrete slabs. *J. Transp. Eng.* **2010**, *136*, 664–677. [CrossRef]
43. Caliendo, C. Delay time model at unsignalized intersections. *J. Transp. Eng.* **2014**, *140*, 04014042. [CrossRef]
44. Astarita, V.; Caliendo, C.; Giofrè, V.P.; Russo, I. Surrogate safety measures from traffic simulation: Validation of safety indicators with intersection traffic crash data. *Sustainability* **2020**, *12*, 6974. [CrossRef]
45. McGrattan, K.; Hostikka, S.; Floyd, J.; McDermott, R.; Vanella, M. *Fire Dynamics Simulator: User's Guide*, 6th ed.; National Institute of Standards and Technology, Fire Research Division, Engineering Laboratory: Gaithersburg, MD, USA, 2019.
46. Xue, H.; Ho, J.; Cheng, Y. Comparison of different combustion models in enclosure fire simulation. *Fire Saf. J.* **2001**, *36*, 37–54. [CrossRef]
47. Korhonen, T. *Fire Dynamic Simulator with Evacuation: FDS+Evac Technical Reference and User's Guide*; VTT Technical Research Centre of Finland: Espoo, Finland, 2018.
48. DiNenno, P.J.; Drysdale, D.; Beyler, C.L.; Douglas Walton, W.; Custer, R.L.P.; Hall, J.R.; Watts, J.M. *SFPE Handbook of Fire Protection Engineering*, 3rd ed.; National Fire Protection Association: Quincy, MA, USA, 1995.
49. Xie, B.; Zhang, S.; Xu, Z.; He, L.; Xi, B.; Wang, M. Experimental study on vertical evacuation capacity of evacuation slide in road shield tunnel. *Tunn. Undergr. Sp. Technol.* **2020**, *97*, 103250. [CrossRef]
50. UPTUN. Workpackage 2—Fire Development and Mitigation Measures. 2008. Available online: https://fogtec-international.com/files/uptun-guideline-08_30.08.07.pdf (accessed on 2 February 2022).
51. CFPA Europe. Fire Safety Engineering Concerning Evacuation from Buildings. Guidelines No 19: 2009. CFPA Eur. 2009. Available online: http://www.cfpa-e.eu/wp-content/uploads/files/guidelines/CFPA_E_Guideline_No_19_2009.pdf (accessed on 2 February 2021).
52. ANAS. Linee Guida per la Progettazione della Sicurezza nelle Gallerie Stradali Secondo la Normativa Vigente. Circolare n°179431/2009. Available online: https://www.stradeanas.it/sites/default/files/pdf/Linee_guida_sicurezza_gallerie_2009.pdf (accessed on 2 February 2022).